

## Article

# A Monitoring System of Sand Mining in Large Rivers and Its Application to the Ayeyarwady (Irrawaddy) River, Myanmar

Charles R. Gruel<sup>1</sup> and Edgardo M. Latrubesse<sup>2,\*</sup> 

<sup>1</sup> Asian School of the Environment and Earth Observatory of Singapore, Nanyang Technological University, Singapore 637551, Singapore; gruelrobin@gmail.com

<sup>2</sup> Environmental Sciences Program-CIAMB, Federal University of Goiás, Goiânia 74690-900, Brazil

\* Correspondence: latrubesse23@gmail.com

**Abstract:** Sand mining is one of the major sustainability challenges of the 21st century. Rates of extraction are surpassing sand supply, and ensuing sand starvation is adversely impacting channel-floodplains and deltas. Therefore, quantifying sand mining's location and extent, through global monitoring and detection, particularly in fluvial systems, is becoming a priority. Sand mining by dredges and barges (extraction of sand and secondarily gravel) in South East Asian rivers, including illegal sand mining, has become rampant, and a monitoring system is not yet in place. Here, we present a high-resolution remote sensing-based mining monitoring system for sand mining in fluvial systems. We used Sentinel-1 mission, a radar component of the Copernicus joint initiative of the European Commission (EC) and the European Space Agency (ESA). The system, tested in the Ayeyarwady, the second largest river in SE Asia, detects sand mining by barges almost in real-time with a satisfactory accuracy level. An additional advantage of the monitoring system is that it does not incur any costs, making it accessible to multiple users, decision-makers, and stakeholders.



**Citation:** Gruel, C.R.; Latrubesse, E.M. A Monitoring System of Sand Mining in Large Rivers and Its Application to the Ayeyarwady (Irrawaddy) River, Myanmar. *Water* **2021**, *13*, 2331. <https://doi.org/10.3390/w13172331>

Academic Editor: Achim A. Beylich

Received: 8 July 2021

Accepted: 19 August 2021

Published: 25 August 2021

**Publisher's Note:** MDPI stays neutral with regard to jurisdictional claims in published maps and institutional affiliations.



**Copyright:** © 2021 by the authors. Licensee MDPI, Basel, Switzerland. This article is an open access article distributed under the terms and conditions of the Creative Commons Attribution (CC BY) license (<https://creativecommons.org/licenses/by/4.0/>).

**Keywords:** sand mining; monitoring system; Ayeyarwady River; Myanmar; Southeast Asia

## 1. Introduction

Sand mining has been defined as one of the major sustainability challenges of the 21st century by the United Nations [1]. Fluvial sands, whose textural characteristics provide the best quality source for various industries and construction, are highly sought after. The current rate of sand and gravel mining in coastal areas and rivers ( $\sim 40,000 \text{ Mt yr}^{-1}$ ) [2] is larger than the estimate of global fluvial sediment discharge ( $19,000 \text{ Mt yr}^{-1}$ ) [3,4]. With extraction exceeding natural renewal [2], demand might outstrip supply by the mid-century [5,6]. Additionally, excessive fluvial sand extraction and ensuing sand starvation exacerbate rivers' vulnerability and their channel-floodplain coupled system and deltas. For example, the decrease in sediment fluxes to the coast alters coastal morphodynamics and habitats [7,8].

The mining of fluvial aggregates (sand, gravel) in Southeast Asia (SE Asia) is exerting enormous pressure on the regional rivers, given regional economies and populations' growth. Research on mining of fluvial aggregates and sediment fluxes in SE Asia has mostly focused on the Mekong River because of its strategic socio-economic and environmental role. Sand flux entering the Mekong River delta has been estimated to be far smaller than the current extraction rates ( $50 \text{ Mt yr}^{-1}$ ) [4].

An additional problem is the proliferation of illegal mining of fluvial aggregates. By 2018, 70 countries had reported illegal fluvial sand extraction [7]. Cambodia, Vietnam, and Indonesia are legal and illicit sand sources in the region [7]. Sand and gravel mining is also increasing in Laos and skyrocketing in Myanmar.

For fluvial aggregates mining to be sustainable, we need to know where, for how long, and what intensity fluvial aggregates have been extracted from Southeast Asian rivers.

Nevertheless, to date, the areas of Southeast Asia impacted by sand mining have not even been systematically identified, and no spatial-temporal analyses have been conducted.

Although sand mining is the most used terminology, the extraction of fluvial aggregates from large rivers can include a dominant grain size population of sand and a proportion of gravel. This article will generically refer to “sand mining”, although the concept includes the dredging and extraction of sand but also secondarily gravel from large river’s beds such as the Ayeyarwady River (also known as Irrawaddy River).

Remote sensing methods are useful tools because they allow monitoring sand extraction on large scales and in areas that are hard to access in time and space. To date, India is the only country in Asia to have implemented a national remote sensing-based Mining Surveillance System (MSS) to monitor illegal mining activities. However, the Indian MSS system does not identify or monitor sand barges dredging fluvial beds, which are the primary means of sand extraction and the cause of environmental concern in Southeast Asian rivers. But sand extraction takes a large diversity of forms and occurs in a variety of physical contexts. Thus, implementing a field-calibrated remote sensing monitoring system capable of detecting, at a high resolution, mining activities in fluvial channels and barges extracting sand from rivers and lakes is crucial for tackling this problem.

Herein, we present a methodology for a high-resolution regional multitemporal assessment of sand mining activities in fluvial systems. We tested the Ayeyarwady River’s surveillance system, the second largest river in Southeast Asia after the Mekong River but though one of the unknown sand mining hotspots in the region, with very few mentions of the sand/gravel extractions in the literature. The choice of the Ayeyarwady River was not arbitrary, as multiple factors make the river a priority for environmental research. It is the fluvial artery that concentrates the majority of the population and GDP of Myanmar, and it is vulnerable to human-made environmental pressure such as mining, dredging, deforestation, and damming. It is also a top priority among the world’s transboundary river basins due to risks related to hydro-political tensions and the lack of water governance at a national level [9].

## 2. Fluvial Aggregates Extraction in Myanmar and the Ayeyarwady River

The Ayeyarwady River stretches for about 2100 km from the Himalayan mountains to the Andaman Sea. The basin drains an area of about 418,000 km<sup>2</sup>, with 91% of the basin located in Myanmar, and 9% is shared with India (Manipur-Nagaland) and China (Yunnan-Xizang) [10] (Figure 1). With a mean annual discharge of ~11,600 m<sup>3</sup>s<sup>-1</sup>, the Ayeyarwady River is the second largest river in SE Asia after the Mekong River in water discharge, and the second or third largest global contributor of wash load to the Oceans [11]. The hydrological regime is monsoonal with floods during the northern hemisphere summer (June–September) and a marked dry season and lower flows in winter (January–March). The discharge reaches an average wet-season maximum of  $3.9 \times 10^4$  m<sup>3</sup> s<sup>-1</sup>. Because of the high seasonality, the mean monthly discharge in August is on average 10 times higher than the discharge in February [11].

The Ayeyarwady River delta is still one of the most pristine in the world, but it is experiencing increasing human-environmental pressure and degradation [12,13], and the system is considered the last largest river of SE Asia to flow relatively freely [11].

Downstream Mandalay, the river alternates anabranching-multichannel alluvial reaches with geologically constrained (nodal zones) segments that are dominated by single-channel patterns. The anabranching reaches are characterized by large fluvial bars and islands. The sediment load of the Ayeyarwady River is still not well quantified. While the suspended load could reach 364 Mt y<sup>-1</sup> [14], and the wash load was estimated in 144 Mt y<sup>-1</sup> [11], the bedload transport of the Ayeyarwady River, the main source of the fluvial aggregates extracted by dredging, has not been systematically assessed. High erosion rates of ~1700 t km<sup>-2</sup>y<sup>-1</sup> in the Chindwin River basin, draining the Indo-Burmese range, and ~1000 t km<sup>-2</sup> y<sup>-1</sup> mainly sourced by erosion of weather gneiss and plutonic rocks in the Upper Ayeyarwady are the main sources of the sediment load (Figure 1) [11,15].

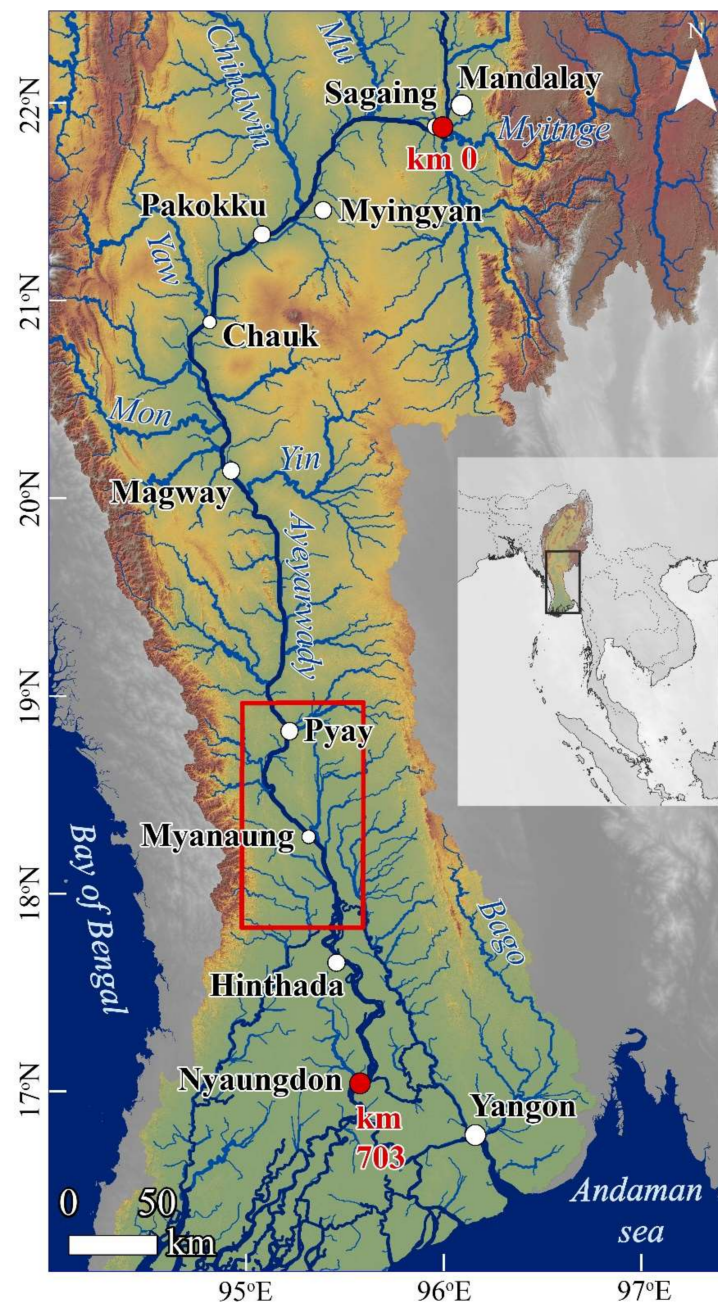


**Figure 1.** The study area of the Ayeyarwady River between Sagaing (km 0) and Nyaungdon (km 703), with the main riparian cities. The red box indicates the reach where ~50% of the detected boats are concentrated (WGS84/UTM zone 46 N).

Because of the size of the river, the monsoonal hydrological regime, and the geomorphologic style of the channel, which is characterized by large and dynamic fluvial bars, it is assumed that the sandy load could represent a significant proportion of the total sediment load. Still, it has yet to be thoroughly quantified.

Sand and gravel in Myanmar are considered natural resources owned by the state. Under Article 37 of Myanmar's 2008 constitution, the Union is the ultimate owner of all lands and natural resources above and below the ground, above and beneath the water, and in the atmosphere. The sand mining industry is regulated through licensing, which is linked to specific tracts within the river. The location of tracks is delineated by geographic coordinates, and the regulation could include limits on the volume of material that can

be extracted [16]. Part of the fluvial aggregates is used for local consumption or large government infrastructure projects, and part is exported [16].

In Myanmar, sand mining management is regulated under the 2006 Conservation of Water Resources and Rivers Law. Operations extracting above 50,000 m<sup>3</sup> have to be assessed for their environmental impact [17].

However, before 2015 there was no limit on the number of suds (about 2.83 m<sup>3</sup>) that could be extracted from the rivers. Since then, two factors have been considered for licenses applications: first, the suitability of the area has to be assessed by the Directorate of Water Resources and Improvement of Rivers (DWIR); second, the boat size each company can operate cannot exceed two boats with a maximum capacity of 30 suds (85 m<sup>3</sup>) each [17].

Fluvial aggregates (sand and gravel) are mined in Myanmar both during the day and at night [17] using various extraction techniques. For example, mixed grain size aggregates are directly excavated from the sand bars during the dry season and stocked on temporary storage-piles, nearby the banks. But the main technique of aggregates mining on the Ayeyarwady River is managed by direct dredging of the river bed using mobile floating structures organized in clusters of dredgers, pushers, and barges. The dredgers extract the aggregates by suction throughout a pipe, sort them, and transfer them to the barges using water as fluid. The barges have variable storage capacity and are moved by pusher boats that can drive one or two attached barges simultaneously toward the main towns or Yangon [16].

### 3. Data and Methods: Sand Mining Monitoring System

A challenge when monitoring fluvial sand mining is that because the extraction concentrates underwater, the surface scars or other visible features used for remote sensing mining-detection of surface mining are not present, boats and barges have to be targeted as indicators of the activity. Furthermore, sand barges' location shifts in time along and across the rivers, once sand supply has been exhausted in a particular reach or once the river shifts and generates new sandy areas. Additionally, adding more complexity, the dynamic character of fluvial mining the diversity of these combined structures (clusterization of barge, dredge, and pusher), make in some cases challenging to identify and characterize a specific remote sensing signature. To tackle the problem, we have implemented a module for sand mining that could efficiently monitor dredging barges along rivers. Similar systems, using radars, have been used to detect ships in areas where fishing is illegal [18]. The methodological procedures are synthesized in Figure 2.

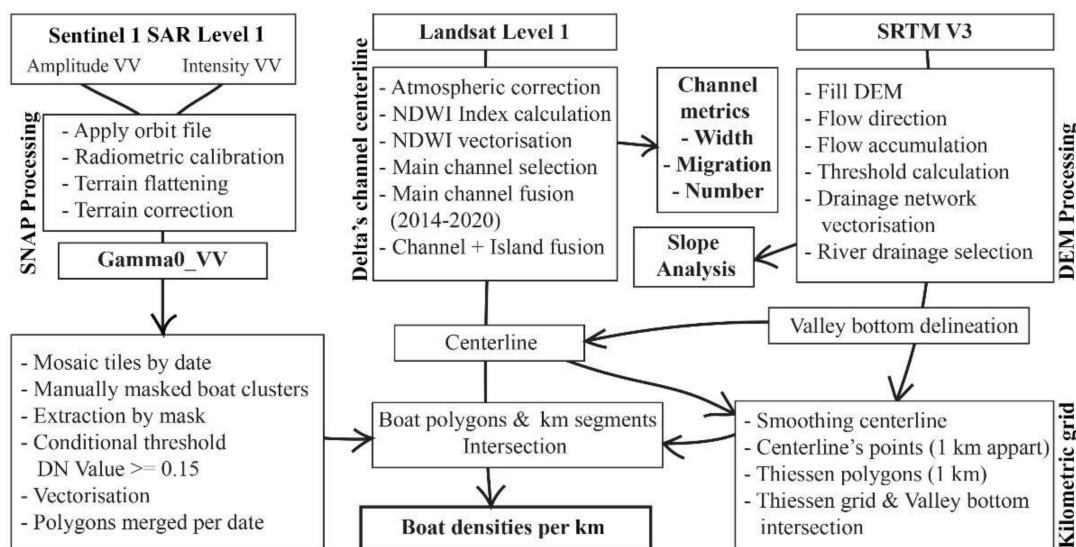


Figure 2. Methodological flowchart.

### 3.1. Imagery Selection

The primary objective was to identify barges effectively throughout the year, regardless of weather constraints such as cloud cover, which substantially limits the use of optical imagery in the tropics, and second, to devise a system that makes use of free imagery. Costly imagery could make the system difficult or even impossible to use in developing countries, where a substantial portion of sand mining from river-beds occurs. To set up the surveillance system, we opted for the Sentinel-1 mission, a radar component of the Copernicus joint initiative of the European Commission (EC) and the European Space Agency (ESA).

We downloaded a total of 500 Ground Range Detected High Resolution (GRD-HR) Sentinel 1 high-resolution products (five tiles by date) available every 12 days between 25 February 2017, and 21 June 2020, from the Copernicus Open Access Hub (<https://scihub.copernicus.eu/dhus/#/home>) (accessed on 19 August 2021). This dataset corresponds to a total of 102 days i.e., 26 dates in 2017, 31 in 2018, 30 in 2019, and 15 in 2020.

Sentinel-1A satellite was launched on 3 April 2014 and the Synthetic Aperture Radar (SAR) free-of-charge has the advantage to be suitable for ship detection, and their resolution is constant, regardless of the distance from the observed targets [19,20]. Sentinel 1 provides a 12-day (ground track) repeated cycle, acquired in Interferometric Wide swath (IW) mode and a 6-day (ground track) repeat cycle for two satellites, with a 250-km swath, a  $20 \times 20$  m spatial resolution, and burst synchronization for interferometry. The incidence angle variation across the swath is between  $29.1^\circ$  and  $46.0^\circ$ . We have chosen the ground range detected (GRD) product processed at Level 1 at high resolution in the ascending orbit because the time visit occurs more often yearlong after the sunset (explanation in “Time Series”).

On the other side, Sentinel 2 optical imagery has a 10-m resolution. They provide more details of objects and a large range of spectral bands than Sentinel 1, notably during the detection and recognition of boats (the distinction between barges and dredgers and the numbers of barges coupled). Unfortunately, the image quality is dependent on the sun elevation angle, the atmospheric conditions, and cloud cover, which is significantly dense in many places of Southeast Asia, where sand mining occurs.

The Sentinel-1 SAR is available in the C band (5.404 GHz central frequency, 5.6 cm of wavelength), and is provided at a single or dual-polarization. Radars equipped with C-band are generally not hindered by atmospheric effects and image through tropical clouds and rain showers. The penetration capability concerning vegetation canopies or soils is limited, restricted to the top layers (sources ESA). On the water bodies, the contrast between the low backscattering of the water and the high signal from the complex and angular structures of the boats, enables a high detection capability of vessels. Because of our small object scale and the 20 m resolution of the radar, the goal was to maximize our detection capabilities and avoid information loss (ex. small boats like dredges). Herein, we pre-processed these images using the ESA Sentinel Applications Platform (SNAP) with radiometric and geometric calibration using SRTM, removing the thermal noise, and georeferenced them into WGS84. Because of the small ship size we targeted and their proximity to each other, we did not apply a speckle filter and multilooking. Instead, after visual inspection and simulations, we applied a minimal threshold of 0.15  $\gamma$  and conversion into a binary raster. After testing different conditions, we selected the Vertical transmission and reception (VV) co-polarization instead of a cross-polarization Vertical transmission Horizontal reception (VH) because of the sharpest signal contrast between the boat and the water. The calibrated backscatter coefficient varies with the incidence angle and polarisation. The incidence angle mainly influences the geometry of vessels in SAR images, and co-polarization generally has a higher value than cross-polarization [20].

Complementary, SRTM, and Landsat images collected from the US Geological Survey (USGS) (<https://earthexplorer.usgs.gov>) (accessed on 19 August 2021) were used for geomorphological mapping. Six Landsat tiles by year using green and infrared bands for the NDWI Index were necessary to cover the studied area.

Water level datasets were sourced by the department of meteorology and hydrology (DMH) of Myanmar (<https://www.moezala.gov.mm/daily-water-level-forecast>) (accessed on 19 August 2021). They are water stage data measured in centimeters at 12:30 p.m. local time.

### 3.2. Boat Types and Detection

The first objective of the system was to set up a method for ship detection. SAR images are commonly used for ship detection on the ocean, and conventional methods generally utilize a constant false alarm detection (CFAR) technique, such as CA-CFAR, OS-CFAR [20]. Ships are mostly made of metallic materials, and they usually have large hulls containing a lot of dihedral and trihedral structures. When detected, ships appear as bright regions in SAR images [20], mainly due to the double reflection of the radar pulses emitted by the sensors [20,21]. The incidence angle is primarily influenced by the geometry of ships in SAR-C images.

The main difficulty encountered on the ocean is related to the texture of the waves, which decreases the contrast between the high backscattering of the ships and the specular reflection of the water body. The high wave rugosity reduces the specular reflection and increases the backscattering. Therefore, it is relatively simple to detect ships at high incidence angles and low wind speeds. Both factors influence the sigma 0 value contrast between the water and the ship [20]. These methods also give the possibility for automatic classifications and measurements to know the size and the surface of the boats.

Applying the same method to detect vessels on rivers like the Ayeyarwady may seem less effective because river barges are smaller, ranging from 40 to 70 m in length and having 400–1200 m<sup>2</sup> of surface area (Figure 3). Also, the mean river channel width is about 1 km during the dry season. However, the fluvial scale and dynamics reduce wave roughness and size, and increase the specular reflection when the surface fluctuation is less than the microwave wavelength (5.6 cm). Under these conditions, the river surface is considered smooth, and radar backscatter appears as a homogeneous background in a SAR image [22], which is particularly advantageous for boat detection on large rivers such as the Ayeyarwady. Of course, limitations still exist. For example, the variety of sizes and types of the river vessels mining the channel or harboring precludes distinguishing between one or multiple vessels. It applies particularly to dredgers, which can be detected only in a cluster. To tackle this limitation, we account for the boat's backscattering surface as a measure itself, understanding that this measure is also dependent on the position of the boat in relation to the satellite angle or the material stored on the deck. However, our goal is not to calculate the exact boat surface but to devise a standardized and reproducible method of detecting vessels on a multi-temporal scale in large tracts of this complex multi-channel river. Since the water body and sand-bars have flat and smooth surfaces and a high specular reflection in band C, the probability of reliably detecting and distinguishing the studied objects (boats) from other objects such as structures on the riverboats anchored to sand bars is also low. Therefore, we have used a Sentinel-2 optical image for each year to ascertain the central channel location during the dry season.

We focused our analysis by filtering the boats located in the mid-channel, as they are detached from the bank and thus identifiable. Barges for transporting goods were distinguished and filtered from sand-mining barges based on sand mining daily activity and based on the mid-channel working or berthing location during the night. As mentioned above, three kinds of vessels are used for sand mining: dredgers, barges, and pushers (Figure 3). The dredgers typically range from 15 to 28 m in length (23 m on average). According to a 2017 survey [16], there are three main classes of dredgers with different storage capacities for sand and gravel extraction. Small dredgers can store from 0.5 to 18 suds, medium-sized dredgers from 20 to 29 suds, and the largest ones can reach up to 30 suds (1 sud = 2.83 m<sup>3</sup>).

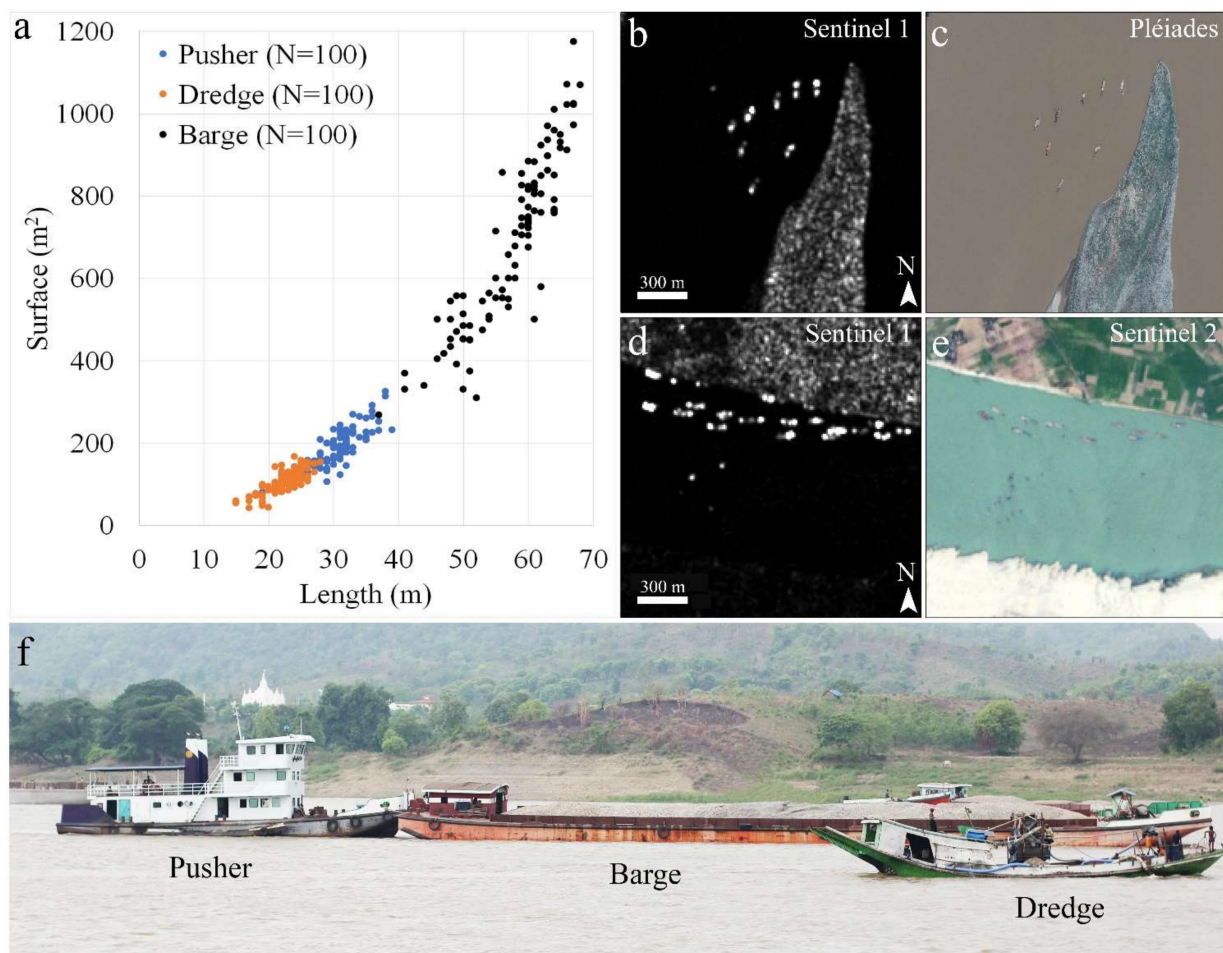


**Figure 3.** (a), Surface and length of individual dredgers, barges, and pushers on the Ayeyarwady River measured from Pléiades satellites at 0.5-m resolution (Google Earth<sup>®</sup>). (b), Sentinel 1 SAR (at 6:15 p.m.) and (c), Pléiades (at 10:51 a.m.) images taken in 1 October 2019 downstream of Thayet (km 410). (d), Sentinel 1 SAR (at 6:16 p.m.) and (e), Sentinel 2 (at 10:39 a.m.) images taken on 10 February 2020 downstream of Tonbo (km 502). In (e), the group of barges (north part) can be distinguished from the clustered dredgers (black dots). (Copernicus Sentinel data 2020, processed by ESA). (f), A pusher, barge, and dredger at Pyay, km 457 (2017).

The comparison between Sentinel-1 SAR (10-m resolution) and Pléiades images (0.5-m resolution) taken on the same day and for boats at the same location shows that Sentinel-1 cannot detect solitary dredgers (which are the core of sand mining activity), and a minimum of three dredgers together is required for the sensor to detect them. The barges can also differ in backscattering power, which is influenced by their size, orientation concerning the satellite swath axis, and the materials stocked on the platform, which either smoothen the surface or increase rugosity. Barge-pusher couples seem to be frequently characterized by two strong (peanut-shaped) backscatter signals (Figure 3b,d), with the first signal from the pusher boat and the second for the barge's bow. There is a weaker backscattering signal from the flat or smooth central part between these extremities, where sand is stored on the flatboat surface. Due to the sharper contrast in the signal between the boats and the water background (Figures 3b,d and 4), we selected vertical polarisation (Gamma VV), rather than vertical and horizontal (Gamma VH). After testing different situations to distinguish the boats from the water without losing the low values (i.e., dredges), we defined the DN value 0.15 as a threshold (Figures 2 and 4).

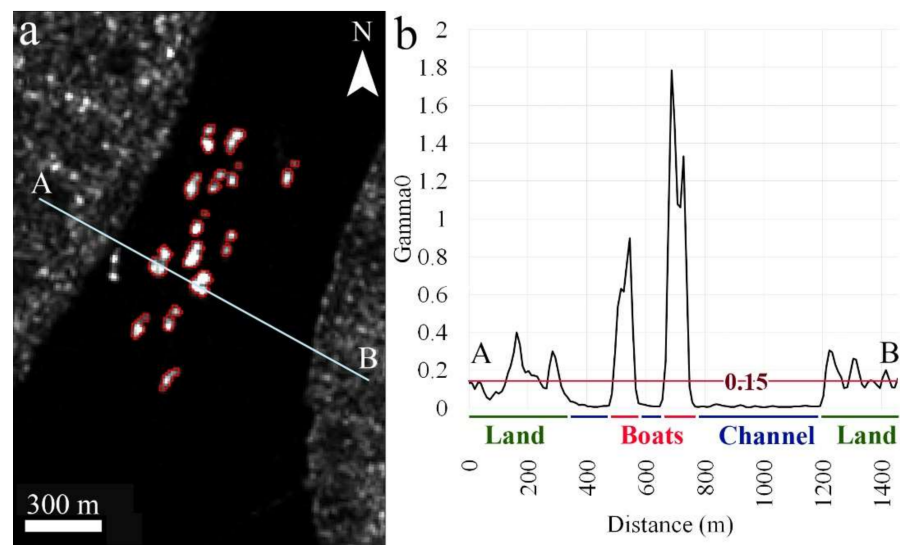


**Figure 4.** (a), Sentinel 1 SAR (Copernicus Sentinel data 2020), barges cluster (km 697, upstream of Nyaungdon), the red lines correspond to the boat delineation according to the 0.15 digital number detection threshold. (b), Signal intensity of the radar image after processing along the A-B cross-section from (a). The 0.15 red line corresponds to the boat threshold used to distinguish pusher-barge and dredge from the water body.

Compared to other monitoring systems on lakes or oceans, the remarkable variability of the fluvial water extension (vertically and laterally) in a shifting river prevents using a single automatically-derived water mask (for automated detection of boats). For that, we delineated manually and extracted by mask each individual or clustered ships before processing the monitoring system.

### 3.3. Time Series

Two satellites' orbit swaths (ascending and descending) are available for the whole length of 703 km, with a visit every 12 days for each orbit. The data allows for synchronic results of the boat activity. However, we selected only the ascending orbit since this satellite track enables imaging of the studied area around 6:15 p.m. (Myanmar time). On this orbit, the satellite reaches the latitude of Mandalay ( $21^{\circ}58' N$ ), the northernmost point of the studied area, after the sunset during 192 days in a year (from 7 September to 18 March), and the southernmost point of the studied area, Nyaugdone ( $17^{\circ}03' N$ ), during 184 days (from 6 September to 9 March). In contrast, in the descending orbit, the satellite images the area around 6.02 a.m., reaching Mandalay ( $21^{\circ}58' N$ ) before the sunrise during 163 days (from 16 October to 28 March), and Nyaugdone ( $17^{\circ}03' N$ ) during 158 days (from 24 October to 31 March).

The selection of the ascending orbit is based on the following rationale. According to the literature [7,17] and field observations, sand mining boats are active day and night or barges storing the mined sand also use to stay anchored in the middle of the channel during the night. In contrast, boats for goods transport are typically anchored in harbors during the night to avoid hazardous navigation. Indeed, the later the image could be taken, the better it could filter and discriminate the sand mining boats from vessels for transport.

Thus, following the sunset and hours of darkness, we selected the ascending satellite orbits. Note that the images are taken from the ascending orbit in the daylight (before the sunset) around 6:15 p.m. (between 9 March and 7 September), which corresponds partly to the rainy season when the boat activity is supposed to be lower.

Our monitoring spans four full calendar years and three full hydrological-mining years (HMY), from 25 February 2017 to 2020, with a complete and regular cover every 12 days. Beyond the selected time series used to set up and test the system, the surveillance system has been implemented to monitor continuously.

### 3.4. Georeferencing of Detected Boats in a Temporally Mobile Alluvial Channel

Like many other large rivers in the world, the Ayeyarwaddy River is, morphogenetically, a mobile system. Thus, systematic multi-temporal monitoring of boats in a dynamic fluvial system faces additional challenges because the river changes in planform through lateral shifting and the generation of new fluvial landforms such as branches, islands, and bars. For that reason, it was not possible to develop a simplified automatic detection system by using a standardized and fixed water mask. The high rate of lateral mobility of the Ayeyarwaddy River at a multi-year and even monthly scale, and the need to compare and normalize the data of occurrence of boats and longitudinal locations, demanded the development and implementation of a kilometer grid breakdown to locate boats as related to the changing morphology of the river. Thus, we created a Thiessen polygons grid following the axis (centreline) of the valley bottom (structural constraint and old terraces) delineation to have a stable referenced geospatial base for studying the whole length and width river changes over time. In our case, the period spans from 1988 (first Landsat images available) to undetermined future years ahead.

The valley was delineated with the Valley bottom tool of the Fluvial corridors tool-box [23] on ArcGIS<sup>®</sup>. It was applied to the Ayeyarwaddy River and its delta using both the river stream and the SRTM DEM (30 m of spatial resolution). The geomorphological characteristics of the valley and maximum flood extent were assessed from S1 C-SAR images during the peak floods of 2015, 2018, and 2019. The river water body from 1988 to 2020 was used to control the lateral mobility, and manual adjustments were also made where the active channel was close to steep slopes and on the narrow stream in rocky controlled nodal reaches. Furthermore, an additional positive 50 m-wide buffer was created around the floodplain boundaries to ensure that the water surface in the narrow zones would be inside these limits.

Because the Thiessen polygon required a defined axis, a centreline was first designed manually along the previously delineated valley bottom and extracted as a frame for determining it. It provides coherence for the river stream multi-year channel delineation. A smoothing tool was used for sharp angles among fluvial reaches, decreasing artifacts of the Thiessen polygons angles to maintain better consistency for multi-temporal comparisons. The grid extends from the Sagaing bridge and was numbered by kilometers, from upstream (km 1) to downstream (Nyaungdon bridge, km 703).

Regarding the procedures described in Sections 3.1 and 3.2, Sentinel 1 Ground Range Detected (level 1) data were first processed using the Sentinel Application Platform (SNAP). The Sentinel 1 dual polarisation VV both Intensity and Amplitude in high resolution, IW mode, were geometrically corrected using SRTM 30 m (1 Arc sec) Digital Elevation Model and projected in the 46N UTM zone. The data were corrected for near-far range incidence angle variations and are thus given as Gamma0 ( $\gamma$ ) values.

Because the main objective is the surveillance of sand mining in almost real-time, after obtaining the Gamma0\_VV images corrected from the SNAP (Figure 2), the five tiles covering the studied area were merged by date. Using the image's displayed in standard deviation, boats (single or clusters) detached from the bank were delineated with polygons and the polygons combined by date. The polygon delineations were used as a mask to extract the boats from the Gamma0\_VV raster mosaic image to isolate the boat backscatter from any other objects. Using the conditional tool, we excluded the values below the DN 0.15  $\gamma$  threshold. The remaining cells corresponding to the boat backscattering were vectorized and then merged by date. To cross the boat entities with their kilometeric locations, we intersected the vectorized boats with the kilometeric grid. The surface calculation in square meters by kilometeric polygon was calculated and exported as a table.

## 4. Discussion and Results

### *Sand Mining in the Ayeyarwaddy River*

The Ayeyarwaddy River hydrological regime is monsoonal, with a flood season spanning from June to September and a low-flow season starting in November. Accordingly, we

use hydrological-mining years (HMY) in our analysis, which span from 1 July to 30 June of the succeeding calendar year. Although sand businesses operate yearlong, extraction is more intensive during the high-water season. The boats' total detected surface displays a correlation with the river's water level, confirming the boats' activity seasonality [16]. Hence, 82% of the boat activity occurs from November to June (Figure 5). Interestingly, activity on 16 April 2019 was particularly low for the period, which could be related to the Thingyan celebration and the day before the Burmese new year (17 April). The radar images were not taken at this festive date but some days before or after for the other years.

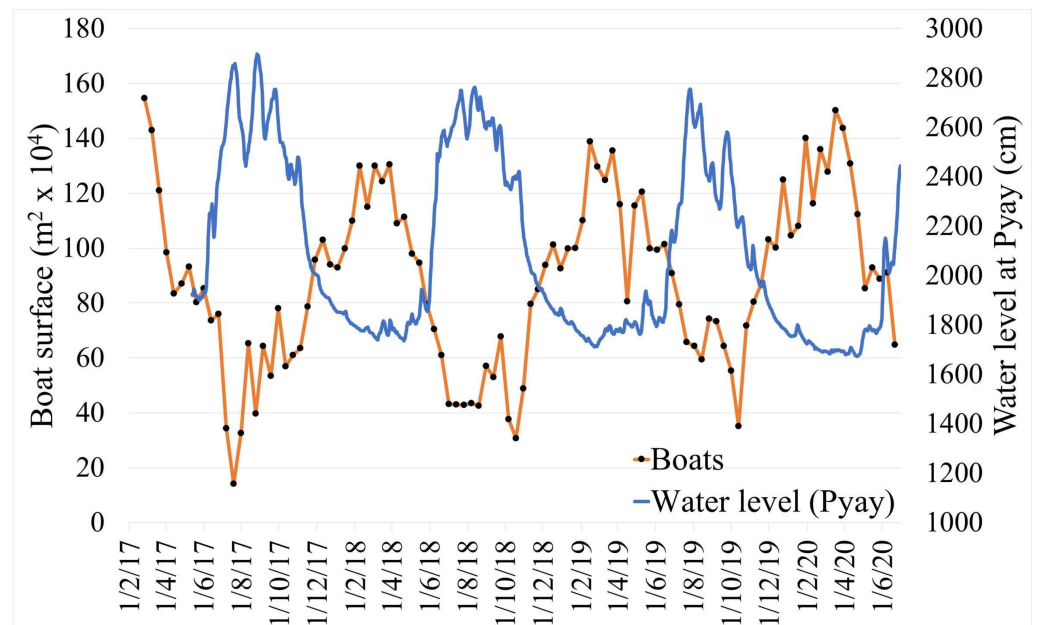


**Figure 5.** Total surface area of detected boats along the study area by date and water level (cm) at the Pyay station Scheme 2017. (source DMH). Although sand businesses operate yearlong, extraction is more intense during the high-water season, and 82% of the sand mining boat activity occurs from November to June.

Boats are detected along the whole ~700-km studied reach, but about 50% of the total concentrate in a short 140 km reach, starting 12 km upstream of Pyay and ending 18 km downstream of Monyo (Figures 1, 6 and 7). This reach, spanning between km 445 and km 586, represents 20% of the whole studied length. Several riparian towns with 20,000 to 135,000 inhabitants are located along the study area. But except for Pyay (~135,000 inhabitants), the six other towns along the reach that concentrates 50% of boats have an average population of ~15,000 inhabitants. This intensively-mined reach is characterized by a plethora of villages and roads leading to the river. Sand is accumulated for distribution in sand piles close to the riverbanks. Observations on the field (2017) and from Google Earth display that the sand piles and loading areas for transferring the sand to the land are usually temporary, with their locations changing from one year to another. Along the reach, we identified 32 sand piles throughout 2014 to 2020 with an average surface area of ~1500 m<sup>2</sup>. About 72% of them (23) were located less than 1 km from the closest main roads. Along this reach, distances by road to Yangon range from 175 to 367 km, while distances to Yangon by boat along the river range from 217 km to 361 km. The most significant concentration of boats is on the main channel. Clusters are also often detected near towns and close to the distribution sites, shifting according to the mining location.

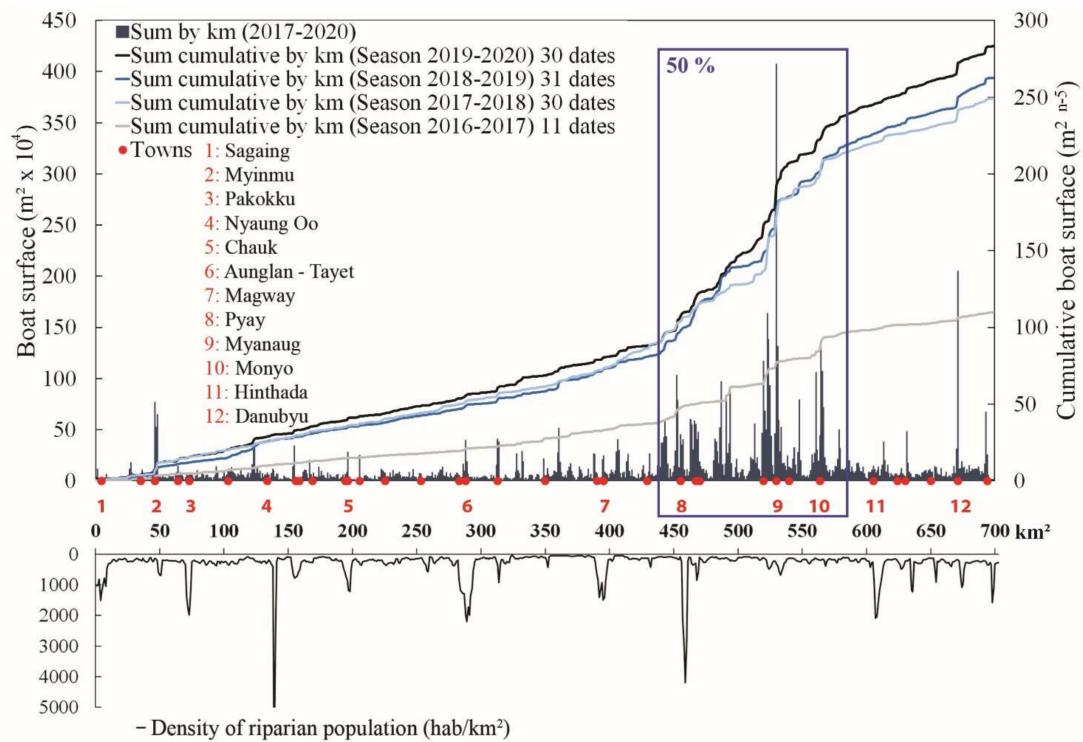


**Figure 6.** Reach from km 1 to 703. The histogram corresponds to the total surface area of boats for all dates by km. The lines indicate the cumulative surface area by hydrological year (HMY, from 1 July to 30 June). Data from 2016–2017 start only on 25 February 2017. The blue rectangle locates the 50% boat concentration between km 445 and km 586. The black bottom line indicates the population’s density within a 5-km radius from the river centerline for the studied reach (source: Census 2014, DOP).

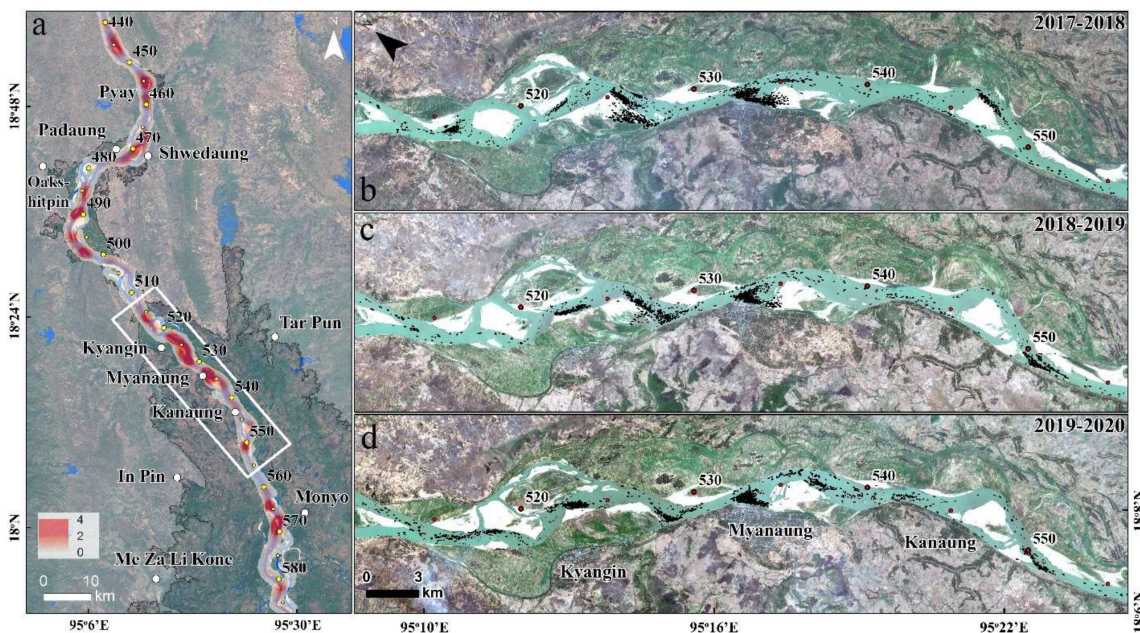


**Figure 7.** (a) The location that concentrates 50% of the boat surface areas from km 445 to 586 and boat density per km (unit of length) and per day within 1-km radius (red gradient) for the whole 2017–2020 period. Only the towns located in the floodplain are displayed. (b–d) correspond to the total boat shape (black areas) location for each HMY, from upstream (km 512) to downstream (km 556) and rectangle location of (b–d), 20 February, 2018, 2019, and 2020 (WGS84/UTM zone 46N) (Copernicus Sentinel data 2020, ESA).

To assess the fluvial reaches with the largest concentrations of boats and their geomorphologic variables and to minimize the noise in the data by removing the transportation vessels, we used the 3rd percentile of boat-sum by date as a threshold filter.

The sand extraction is more intensive in river reaches that temporarily sustain one channel and episodically two. Narrow nodal points, where the channel widths are less than 600 m, are not favorable to sand-bed extraction because of the structural-rocky control and the hydrodynamic conditions that constrain the development of a well-structured mobile sandy bed. The concentration of sand mining activities does not correlate with the increase in migration rates or river width. River branching increase does not appear to be a factor influencing sand mining activity because, in multibranching reaches, fluvial activity still concentrates on the main channel and the head of some fluvial bars (Figure 7).

During the three HMYs, boats showed a similar longitudinal distribution pattern and frequency. The long river reach from Mandalay (km 1) to around Pyay (km 458) had a constant low boat density. A localized spot of higher boat activity was around Myinmu (km 47). However, along the reach, the numbers of boats were closely linked to towns, suggesting berthing or local transportation (Figures 6 and 7a).

However, along the further 141 km river reach, from km 445 (upstream of Pyay) to km 586 (downstream of Monyo), boat activity was massive during all the HMYs (Figures 6 and 7a). In the 2017–2018 HMY, the boat surface area in this section (141 km) was 2.3 times larger than in the upstream reaches and was more than 2.5 times larger than upstream during the 2018–2019 and 2019–2020 HMYs. Downstream, in Danubyu town (km 675), local activity was also intensive in the three HMYs (Figure 6).

The general activity of boats and mining along the whole 703-km study area suggests that mining activity in 2019–2020 was higher than the two previous HMYs.

## 5. Concluding Remarks

A global program for detection and monitoring of sand mining has been regarded as crucial for quantifying the location and extent of sediment mining and the natural variations in sand flux in the world's rivers [1,6,7,24].

Thus, our outcomes are relevant for both efforts: (a) the design and implementation of a field-calibrated remote sensing detection and monitoring system of sand mining that can be applied worldwide; (b) specifically for Myanmar, where access to data and field works is difficult, the monitoring and information we developed allow to understand the spatial-temporal distribution and level of intensity of sand mining in the Ayeyarwady River, a strategic fluvial basin in Southeast Asia. Sand mining in the Ayeyarwady River requires close monitoring as excessive sand extraction can affect the morphodynamic balance, the sediment budgets of the fluvial belt, and negatively impacts the supply of sediments to the delta.

Our monitoring system demonstrates to be capable of detecting sand mining locations on large rivers and cloudy tropical areas in almost real-time, accurately, and free of charge, making it accessible to a range of users, decision-makers, and stakeholders such as government agencies, environmental organizations, NGOs and local communities.

**Author Contributions:** E.M.L. and C.R.G. jointly conceived the study, designed the methodology, and participated in field activities. C.R.G. processed the remote sensing products. C.R.G. and E.M.L. analyzed the data and wrote the article in collaboration. All authors have read and agreed to the published version of the manuscript.

**Funding:** This research was funded by the Earth Observatory of Singapore and Asian School of the Environment, Nanyang Technological University.

**Institutional Review Board Statement:** Not applicable.

**Informed Consent Statement:** Not applicable.

**Data Availability Statement:** The data presented in this study is available on request from the corresponding author.

**Conflicts of Interest:** The authors declare that they have no known competing financial interests or personal relationships that could have appeared to influence the work reported in this paper.

## References

1. UNEP. *Sand and Sustainability: Finding New Solutions for Environmental Governance of Global Sand Resources*; United Nations Environment Programme: Geneva, Switzerland, 2019.
2. Peduzzi, P. Sand, rarer than one thinks. *Environ. Dev.* **2014**, *11*, 208–218.
3. Milliman, J.D.; Farnsworth, K.L. *River Discharge to the Coastal Ocean: A Global Synthesis*; Cambridge University Press: Cambridge, UK, 2011.
4. Hackney, C.R.; Darby, S.E.; Parsons, D.R.; Leyland, J.; Best, J.L.; Aalto, R.; Nicholas, A.P.; Houseago, R.C. River bank instability from unsustainable sand mining in the lower Mekong River. *Nat. Sustain.* **2020**, *3*, 217–225. [[CrossRef](#)]
5. Sverdrup, H.U.; Koca, D.; Schlyter, P.A. Simple system dynamics model for the global production rate of sand, gravel, crushed rock and stone, market prices and long-term supply embedded into the WORLD6 model. *Biophys. Econ. Resour. Qual.* **2017**, *2*, 8. [[CrossRef](#)]
6. Bendixen, M.; Best, J.; Hackney, C.; Iversen, L.L. Time is running out for sand. *Nature* **2019**, *571*, 29–31. [[CrossRef](#)] [[PubMed](#)]
7. WWF. *Uncovering Sand Mining's Impacts on the World's Rivers*; World Wildlife Fund for Nature: Morges, Switzerland, 2018.
8. Best, J. Anthropogenic stresses on the world's big rivers. *Nat. Geosci.* **2019**, *12*, 7–21. [[CrossRef](#)]
9. TWAP. United Nations Environment Programme (UNEP). *Transboundary River Basins: Status and Trends. Summary for Policy Makers*. 342. 2016. Available online: <http://www.geftwap.org/publications/river-basins-spm> (accessed on 19 August 2021).
10. Gruel, C.R. Sédimentation et érosion dans le delta de l'Ayeyarwady, Focus sur trois archipels situés sur le cours principal du fleuve. In *Technical Report for IRD; Deltas of South East Asia*: Villeneuve-les-Avignon, France, 2018; p. 221.
11. Latrubesse, E.; Park, E.; Kastner, K. The Ayeyarwadi River (Myanmar): Whasload transport and its global role among rivers in the Anthropocene. *PLoS ONE* **2021**, *16*, e0251156. [[CrossRef](#)] [[PubMed](#)]
12. Syvitski, J.P.M.; Kettner, A.J.; Overeem, I.; Hutton, E.W.H.; Hannon, M.T.; Brakenridge, G.R.; Day, J.; Vörösmarty, C.; Saito, Y.; Giosan, L.; et al. Sinking deltas due to human activities. *Nat. Geosci.* **2009**, *2*, 681–686. [[CrossRef](#)]
13. Chen, D.; Li, X.; Saito, Y.; Liu, J.P.; Duan, Y.; Liu, S.; Zhang, L. Recent evolution of the Irrawaddy (Ayeyarwady) Delta and the impacts of anthropogenic activities: A review and remote sensing survey. *Geomorphology* **2020**, *365*, 107–231. [[CrossRef](#)]
14. Robinson, R.A.J.; Bird, M.I.; Oo, N.W.; Hoey, T.B.; Aye, M.M.; Higgitt, D.L.; Lu, X.X.; Swe, A.; Tun, T.; Win, S.W. The Irrawaddy river sediment flux to the Indian ocean: The original nineteenth-century data revisited. *J. Geol.* **2007**, *115*, 629–640. [[CrossRef](#)]
15. Garzanti, E.; Wang, J.G.; Vezzoli, G.; Limonta, M. Tracing provenance and sediment fluxes in the Irrawaddy River basin (Myanmar). *Chem. Geol.* **2016**, *440*, 73–90. [[CrossRef](#)]
16. WWF Greater Mekong. *Sediments and geomorphology of the Ayeyarwady*. In *Ayeyarwady State Of the Basin Assessment (SOBA)*; WWF Greater Mekong: Bangkok, Thailand, 2017.
17. Kadoe, B. *Exploring Sand Mining in Yangon, Myanmar: Status, Regulations and Impacts, Practitioner Report*. Ph.D. Thesis, Clark University, Worcester, MA, USA, 2018.
18. Kurekin, A.A.; Loveday, B.R.; Clements, O.; Quartly, G.D.; Miller, P.I.; Wiafe, G.; Agyekum, K.A. Operational monitoring of illegal fishing in Ghana through exploitation of satellite earth observation and AIS data. *Remote Sens.* **2019**, *11*, 293. [[CrossRef](#)]
19. Oliver, C.; Quegan, S. *Understanding Synthetic Aperture Radar Images*; SciTech Publishing: Chennai, India, 2004.
20. Wang, Y.; Wang, C.; Zhang, H.; Dong, Y.; Wei, S. A SAR Dataset of ship detection for deep learning under complex backgrounds. *Remote Sens.* **2019**, *11*, 765. [[CrossRef](#)]
21. Crisp, D.J. The state-of-the-art in ship detection in Synthetic Aperture Radar imagery. *Org. Lett.* **2004**, *35*, 2165–2168.
22. Huo, W.; Huang, Y.; Pei, J.; Zhang, Q.; Yang, J. Ship detection from Ocean SAR Image based on local contrast variance Weighted Information Entropy. *Sensors* **2018**, *18*, 1196. [[CrossRef](#)] [[PubMed](#)]
23. Roux, C.; Alber, A.; Bertrand, M.; Vaudor, L.; Piégay, H. "FluvialCorridor": A new ArcGIS toolbox package for multiscale riverscape exploration. *Geomorphology* **2015**, *242*, 29–37. [[CrossRef](#)]
24. Bendixen, M.; Iversen, L.L.; Best, J.; Franks, D.M.; Hackney, C.R.; Latrubesse, E.M.; Tusting, L.S. Sand, gravel, and UN Sustainable Development Goals: Conflicts, synergies, and pathways forward. *One Earth* **2021**, *4*, 1095–1111. [[CrossRef](#)]